Coastal Hazards and the Global Distribution of Human Population

CHRISTOPHER SMALL,* VIVIEN GORNITZ,‡ and JOEL E. COHEN§

*Lamont-Doherty Earth Observatory of Columbia University, Palisades, NY 10964
‡Center for Climate Systems Research, Columbia University and Goddard Institute for Space Studies, National Aeronautics and Space Administration, 2880 Broadway, New York, NY 10025
§Rockefeller University and Columbia Earth Institute and School of International and Public Affairs, 1230 York Ave., Box 20, New York, NY 10021-6399

ABSTRACT ●

A frequently predicted consequence of global climate change is an increased effect of coastal hazards on the world's human population. The impact of coastal hazards depends on the proximity of human population to the coastal zone. Recently compiled population estimates are combined with a new continental digital elevation model in an attempt to quantify the global distribution of human population and occupied land area with respect to elevation and coastal proximity. The limited spatial resolution of the census data allows one to quantify some of the uncertainty in the spatial distribution of population. This provides a lower bound on the uncertainty in the resulting distributions but does not account for uncertainty in the census data or elevation data. Long-term records of relative sea level rise, tidal heights, and storm surge heights can be combined with global sea level rise estimates for a variety of climate change scenarios to estimate the approximate magnitude of vertical changes in local sea level. It is verified that large numbers of people live at low elevations near coasts but the uncertainties are too large to provide meaningful estimates of the number of people who reside in so-called "coastal zones" worldwide. The principal conclusion is that both the spatial distribution and the resolution of global data must be significantly improved before realistic quantitative assessments of the global impact of coastal hazards can be made.

Key Words: coastal, global, hazard, population, sea level rise, uncertainty.

INTRODUCTION ●

It is well known that the world's coastal regions are generally more heavily populated than are the continental interiors. Eleven of the world's 15 largest cities are located on sea coasts or estuaries (Cohen and Small, 1998). Estimates of the proximity of population to coastlines vary widely because of ambiguity in the definition of "coastal" (Cohen et al., 1997). Populations living at low elevations near coasts are frequently mentioned in discussions of sea level rise (SLR) and coastal hazards (e.g., Intergovernmental Panel on Climate Change [IPCC], 1996b; Nicholls and Leatherman, 1995), but the number and nature of their distribution have not been quantified accurately on a global basis.

The purpose of this study is to quantify what is currently known about global distributions of population and land area with respect to elevation and coastal proximity and to discuss implications for changes in global sea level and coastal hazards. It has been estimated that global warming may increase rates of SLR by two to five times present rates (IPCC, 1995a). It has also been proposed that a climate-induced collapse of the West Antarctic ice sheet could raise global sea level by 4–6 m (Oppenheimer, 1998). Land areas located at low elevations within several meters of present mean sea level would be at risk of submergence and more frequent flooding by storm surges. However, the projected SLR will not be spatially uniform because of vertical land movements and dynamic changes in atmospheric pressure and ocean currents. As far as coastal hazards are concerned, the relative, or local, SLR (RSLR) is of greater importance than is a global mean value. Even in the absence of significant changes in global sea level, climate-induced changes in coastal storm frequency or severity would have implications for coastal populations.

Several previous studies have attempted to assess the global populations at risk from SLR. The Coastal Zone Management Subgroup of the IPCC (Houghton et al., 1992) used a Common Methodology—a sequence of seven steps intended to provide a common basis for a worldwide assessment of coastal vulnerability to a 1-m SLR by the year 2100. Results for 23 country case studies were summarized in IPCC (1996b; see also Nicholls and Leatherman, 1995). In addition to these case studies, Hoozemans et al. (1993), applying the Common Methodology, estimated an increase in the global population at risk from annual flooding as a result of a 1-m SLR from 47–61 million people, at present population levels, and to 100 million after 30 years of growth. Their study was based on data including, among others ETOPO5 Elevation, Global Wave Statistics, Admiralty Tide Tables (London), World Population Projections (1989–1990), and the *Times*

Atlas of the World. Since these studies were conducted, new sources of population and elevation data have become available at higher spatial resolutions than previously.

In this study, currently available information about global distributions of population and land area are integrated with respect to elevation and coastal proximity, and the uncertainty associated with spatial combinations of these data is assessed. By using the most detailed global population, elevation, and coastline data sets publicly available, the implications of the resulting distributions with respect to a global compilation of local relative SLR data for different climate change scenarios are considered. Although global analyses are obviously lacking in the important detail provided by local studies, they can provide a synoptic perspective that would be difficult to obtain from the diversity of approaches and foci of local and regional analyses. The objective here is not to provide precise estimates of population or land area at risk but rather to summarize the global relationships between population and continental physiography and to discuss their implications for coastal hazards and different SLR scenarios. A subsidiary objective is to identify improvements in data required to achieve the major objective more precisely.

POPULATION DATA

The human population distribution used in this study was compiled by Tobler et al. (1997) and was based on censuses from 217 countries partitioned into a total of 19,032 secondary administrative subdivisions (corresponding to counties in the United States). The census years ranged from 1979–1994. Tobler et al. (1997) estimated the 1994 populations of these 19,032 polygons by projecting from the census years to 1994. All subdivisions in each country were assumed to change exponentially at the same rate. The total 1994 population estimated in this way was 5,617,519,139 people. The uncertainty of this estimate probably exceeds 2%, based on the uncertainty of censuses in developed countries. The 19,032 polygons totaled 132,306,314 km^2, 25.9% of the world's surface area (5.096×10^8 km^2) and 99.5% of ice-free land ($\sim 1.33 \times 10^8$ km^2). The average population density of occupied land in these data is 42.45 people/km^2. The average polygon area is $\sim$6950 km^2 and the average number of people per polygon is $\sim$295,000.

Assuming a uniform spatial distribution of population within each polygon, Tobler et al. (1997) used these data as the basis for a mass conserving spatial redistribution to produce unsmoothed gridded population estimates [http://www.ciesin.org/datasets/gpw/globldem.doc.html] of 2,003,971 quadrangles at 5-arc-min (5′) resolution (Fig. 1). This corresponds to squares 9.3 km on a side at the equator and diminishing in width with poleward latitude. The errors introduced by the assumption of a uniform population density within each polygon are distributed unequally over space, depending on the local spatial resolution and quality of census data. In addition to the exclusion of Antarctica and Greenland, some low lands in the Canadian arctic were not included in these quadrangles. The total number of people in the unsmoothed gridded model was 5,622,166,374, larger than was the total population calculated from the original 19,032 points by 0.083%. This discrepancy is believed to result from the gridding procedure (W. Tobler and U. Deichmann, 1997, personal communications) but is significantly smaller than is the expected error in the original population estimates. The occupied quadrangles totaled 129,674,365 km^2, 25.4% of the world's surface area and 97.5% of ice-free land.

CONTINENTAL ELEVATION AND COASTLINE DATA

Continental hypsography was derived from global, 30-arc-sec (30", $\sim$1 km at the equator) gridded elevations provided by the Earth Resources Observation Systems Data Center, Sioux Falls, South Dakota (http://edcwww.cr.usgs.gov/landdaac/landdaac.html). The 30" elevation model was derived from Defense Mapping Agency digital terrain elevation data Level 1 (3") gridded topography as well as from data from several other international mapping agencies (including those of Japan, Mexico, and New Zealand). The gridded topography covered North and South America, Africa, Europe, Asia, Australia, Oceania, Greenland, and Antarctica.

Coastal proximity was calculated as distance to the nearest coastline at each point for which a population estimate was available. The coastline is based on the Global Self-consistent Hierarchical High Resolution Shoreline (Wessel and Smith, 1996) digital coastline file, consisting of 10,390,243 points worldwide. Because distances were calculated for a uniform 5′ grid, the cells containing coastline points are assigned a proximity of 0 km, whereas proximities of interior grid cells are based on the distance from the centroid of the interior cell to the centroid of the nearest coastal cell. This introduces an error of less than one grid cell to the proximity estimates. This introduced uncertainty is accepted because the emphasis of this study is on global distributions rather than on precise estimates of coastal populations and because the spatial uncertainties in the population distributions are significantly larger.

The demographic and hypsographic data were coregistered by calculating the median of the 30" elevations within each 5′ quadrangle for which a population estimate was available. Population density for each quadrangle was estimated but did not account for differences in the fractional land area of quadrangles on coastlines; in these areas, population densities are minimum estimates.

SEA LEVEL DATA

The sea level data come from a worldwide network of over 1700 tide-gauges, with some records going back >100

years (Spencer and Woodworth, 1993). Analysis of tide-gauge data shows an absolute SLR at a rate of 1–2.5 mm/yr over the past 120 years (IPCC, 1996a). The average trend for eastern North America and several other regions (western Europe, Australia, and New Zealand) is ~1.5 mm/yr (Gornitz and Seeber, 1990; Gornitz, 1995a). This is slightly lower than the global value of 1.8 mm/yr used by the IPCC (1996a; Douglas, 1991).

Many factors influence sea level. Tide-gauges record fluctuations due to changes in atmospheric pressure, ocean currents, tides, and vertical land movements, including glacial and hydro-isostasy, tectonism, subsidence of major deltas due to sediment compaction, groundwater pumping, and other mass fluxes. Vertical crustal motions are a major source of spatial variability in sea level (Gornitz, 1995b). In addition, sea level varies in response to dynamic factors, including steric changes (in temperature or salinity), currents, and coupled oceanographic-atmospheric forcing (e.g., the El Nino-Southern Oscillation or the Northern Atlantic Oscillation).

The RSLR is calculated as the slope of the least squares linear regression through the annual mean sea level data for each tide-gauge station. A 30-year record length is taken as a minimum to insure a reliable trend and widespread geographic coverage. A total of 246 stations meet the following minimal criteria: 30 years of data, a completeness ratio of >50% (number of years of data/total record length), and a standard error on the trend of <0.7.

SEA LEVEL RISE

There are several ways in which global climate models are used to calculate SLR. For example, the IPCC IS92a "best estimate" projection is based on a one-dimensional upwelling-diffusion model to calculate thermal expansion, a global glacier melt model for mountain glaciers, and the use of static sensitivity values for the Greenland and Antarctic contributions, which ignore any dynamic response. The Goddard Institute for Space Studies (GISS) ocean-atmospheric General Circulation Model (GCM) includes ocean convection, vertical diffusion, and bottom friction. The mass balance of the crysosphere is calculated by differencing snowfall and ice melt. Glacial ice transport is simulated for Antarctica but not for Greenland or mountain glaciers. Four scenarios in this study are considered below.

1. Extrapolation of current trends. The first scenario assumes no climate change and simply extrapolates current rates of local SLR from 1990–2100.
2. Goddard Institute for Space Studies General Circulation Model. The GISS coupled ocean-atmosphere GCM (Hansen et al., 1983, 1988; Russell et al., 1995) simulates the earth's climate in three dimensions at 4° × 5° horizontal resolution and calculates ocean height (i.e., sea level) directly.

   Two GCM runs are presented. In the greenhouse gas (GG) run, inputs to the atmosphere of greenhouse gases are increased by 1% annually, but sulfate aerosol inputs remain constant at 1989 values. To minimize effects of model drift, the SLR projections are based on the differences between the greenhouse gas projections and a control run, which uses present day climate. Sea level data have been averaged in decadal intervals, starting in 1990, to minimize the effects of interannual variations.

   In the greenhouse gas + sulfate aerosols (GS) run, atmospheric inputs of greenhouse gases are increased by 1%/yr and sulfate aerosol inputs increase annually until the year 2050, with a slight decrease thereafter. The results represent differences between greenhouse gas and sulfate projections and a control run, with current climate, in decadal averages.
3. GISS/GCM. The GISS GCM SLR projections may underestimate SLR, because the simulations are assumed to be in radiative equilibrium at the beginning of the runs (i.e., in 1990). In reality, several decades may be needed to establish this equilibrium. This leads to a lower projected global warming (and associated SLR) than the final equilibrium value (the "cold start" problem). On the other hand, the forthcoming IPCC scenarios will assume a lower than 1%/yr rise in greenhouse gases, which would reduce the SLR from earlier estimates.
4. IPCC IS92a simulation. The IPCC 1995 "best estimate" includes changes in sulfate aerosols. Assumptions of population growth, energy use, and greenhouse gas emissions are given in Houghton et al. (1992). More recent IPCC global temperature and SLR projections will probably be lower that their previous estimates, but the new results have not yet been officially published. Thus, the two GISS GCM runs may turn out to be comparable with the latest IPCC projections.

In addition to permanent inundation due to accelerated sea level rise (ASLR), the coast is at risk of flooding from storms. The total height Hf of a flood with frequency of occurrence f (e.g., f is annual or the 100-year flood) is equal to the sum of the projected ASLR for the year t for each SLR scenario, the flood surge (SURGE), mean high water (MHW), and the rate of land subsidence or uplift (SUBS).

Hf is computed for specific points in time. The ASLR term depends on t and on the scenario, SURGE depends on f, SUBS depends on RSLR and t, with MHW remaining constant. Surge levels are assumed to remain constant over time (i.e., no change in frequencies and intensities of coastal storms). Surge levels are taken from Hoozemans et al., 1993 (table A-1). These represent country-wide average return intervals of 1, 10, 100, and 1000 years (or coastal averages for countries with more than one coast). The flood level is maximum at the time of high tide. Mean high water is half the

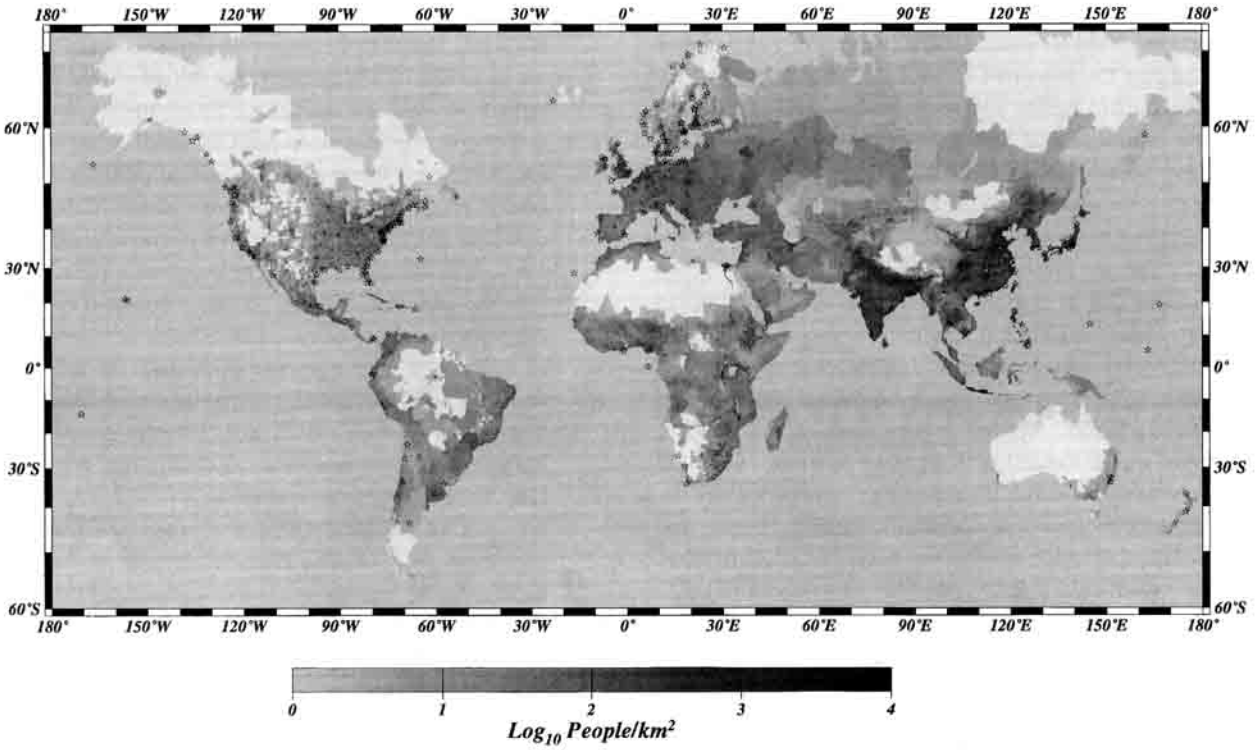

Figure 1: Global population density (from Tobler et al., 1997) and locations of 246 long-term sea level monitoring stations (stars). This image does not show the full detail of the gridded population density but emphasizes the sparse population of the continental interiors relative to the denser population of the coasts. Population density is shown on a Log_{10} scale. The majority of sea level monitoring stations are located in Europe, Japan, and North America, but many of the higher population densities near coastal areas are in southern and eastern Asia.

mean tide range at each tide gauge station (National Oceanographic and Atmospheric Administration (NOAA) 1995). It is assumed that a constant rate of subsidence gives a level of subsidence that is a linear function of time. To conform with the convention for sea level, SUBS indicates subsidence if positive (apparent SLR—land sinking), and uplift, if negative (apparent sea level fall—land rising). This convention is the opposite of that commonly used by geologists and geodesists.

The spatial distribution of long-term monitoring stations heavily favors Europe, Japan, and North America and does not provide adequate coverage for a global assessment of coastal inundation. By including additional stations with shorter or less complete temporal coverage, the distribution improves somewhat but is still lacking in a number of heavily populated regions, particularly in southern Asia. In spite of the shortcomings of this spatial distribution, the vertical distribution of flood heights may provide some useful information if its variability is representative of the global distribution. Figure 2 indicates that the magnitude of local

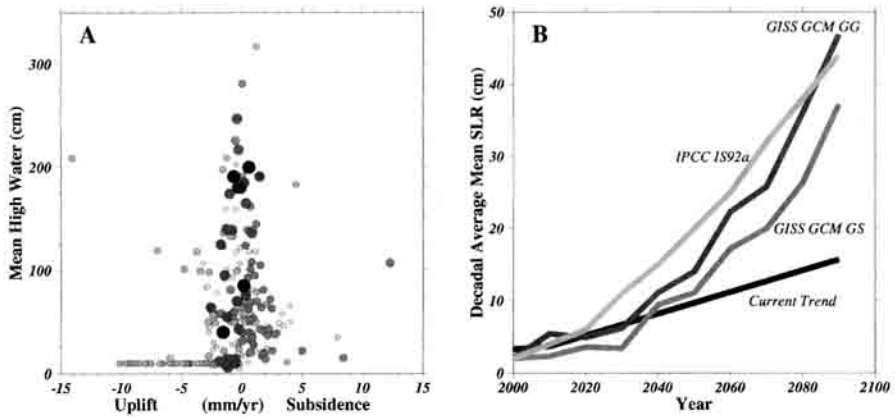

Figure 2. Historical SLR data and 100-year model scenarios. (A) Subsidence and mean high water for 246 long-term sea level monitoring stations. Mean high water is generally <3 m above mean sea level. Extrapolation of current subsidence rates of these stations would generally result in significantly less than 1 m of subsidence over the next 100 years. Size and shading of symbols represents Hoozemans et al. (1993) estimates of 100-year surge heights, ranging between 0 m (small, light grey) and 6 m (large, black). The large number of stations showing uplift is a result of the numerous sea level stations in Scandinavia and Alaska currently experiencing post-glacial rebound and in Japan experiencing tectonic uplift. (**B**) Mean SLR scenarios discussed in the text show similar increases and suggest ~50 cm of SLR over the next 100 years.

RSLR is generally greater than is the magnitude of global SLR projected by the scenarios considered here and that the magnitude of historic surge heights is larger still. As pointed out above, regional coastal subsidence and spatial variability in atmospheric and tidal effects controlling RSLR are often of greater importance than is the projected ASLR. Figure 2 indicates that RSLR is comparable with ASLR but tidal heights and storm surges are several times greater. Regional coastal oceanography and meteorology also play important roles in determining the height and impact of storm surges. The importance of local effects in determining inundation potential emphasizes the need for improved spatial distribution of sea level monitoring stations.

SPATIAL UNCERTAINTY OF POPULATION DISTRIBUTION

The limited spatial resolution of the population data introduces quantifiable uncertainty in the distributions considered in this analysis. There are additional uncertainties related to the accuracy of both the population data and geophysical data but these are considerably more difficult to quantify. The mass-conserving gridding operator used by Tobler et al. (1997) to convert the population data to a uniform grid assumes that the total population of each district is uniformly distributed within the area of the district. Although this is generally unlikely, it does represent one extreme of the set of all possible spatial distributions of the specified population within the district. The other extreme would be the maximal clustering represented by the entire population occupying a single location within the district with the rest of the district being uninhabited. The population density would depend on the size of the location into which the population was packed. This maximal clustering condition has a number of possible manifestations depending on where within each district the maximum density point occurs. If a finite spatial resolution is specified, then it is possible to calculate a finite number of realizations of this condition and determine which one results in maximal clustering at a global scale. In reality, both of these extremal conditions probably represent exceedingly unlikely occurrences. However, knowing the extremal bounds is useful because it brackets the range of possible occurrences.

The distribution of district areas for the 19,032 census estimates gives an indication of the spatial resolution of the population data (Figure 3). Because we know the area but not the specific boundaries (not published by Tobler et al. [1997] because of copyright restrictions) for each district, we will consider units of characteristic resolution defined as the square root of the area of the district. The median characteristic resolution for census districts in this data set is 35.5 km. The median characteristic resolution of people (using people rather than census districts as the units of analysis) is 63 km. These figures give some indication of the spatial uncertainty for global analyses. The designation of census districts tends to favor spatial resolution because district size generally diminishes with increasing population density. In the data set used here, the highest densities occur at the smallest spatial scales and maximum density diminishes consistently with increasing district size. Although the correlation between population density and characteristic resolution is only -0.38, almost all (798 of 832) of the districts with population densities >1000 people/km^2 had characteristic resolutions of <50 km and the maximum characteristic resolution of these is 89 km. The median dis-

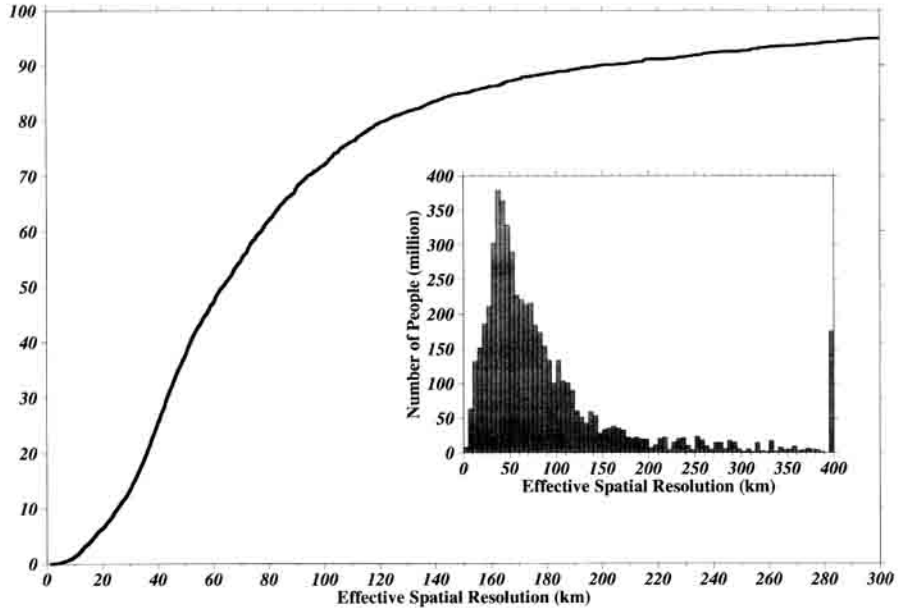

Figure 3: Distributions of spatial resolution of global population data set compiled by Tobler et al. (1997). Inset histogram shows distribution of effective spatial resolutions (square root[area]) of 19,032 census estimates used in this study. One half of the units are <35.5 km in linear dimension but these units contain $<20\%$ of the global population. Cumulative distribution (the integral of the histogram) shows the percentage of the world's population that can be located to within a given distance using these data. For example, the location of 50% of the world's population is known to within 63 km and 72% to within 100 km.

trict population in this data set is 49,494 people and the median density is 52 people/km^2.

The effect of spatial uncertainty is most pronounced on proximity estimates because they depend entirely on the spatial distribution. The effect of spatial uncertainty on other spatially varying parameters depends on the spatial variability of the particular parameter. For example, if the elevation does not vary significantly within the area of a district, then neither the size of the district nor the distribution of the population within the district affects the distribution of population with respect to elevation in the district. On the other hand, if elevation varies widely within a district, the spatial distribution of the population has a large influence on its distribution with respect to elevation. In this analysis, the spatial uncertainty is considered to be one half the characteristic resolution, representing the average distance from the centroid to the boundary of an arbitrarily shaped census district. Figure 4 shows the distribution of spatial uncertainties for the 19,032 census districts with respect to coastal proximity. Although the uncertainty is smallest for the coastal districts, it is still substantial relative to any reasonable estimate of coastline incursion. This uncertainty is too large to make meaningful quantitative statements about the number of people globally at risk from the kinds of coastal hazards considered here.

GLOBAL PATTERNS OF POPULATION DISTRIBUTION

The global distribution of population relative to elevation and coastal proximity can provide some indication of the extent to which low coastal regions are populated relative to the interiors of the continents. Even with the uncertainties discussed above, a quantitative assessment of the available data may indicate which regions should be the focus of more detailed study and data collection. These distributions (Figure 5) show the scale over which global population diminishes with increasing elevation and distance from coastline. The elevation distribution shown here is a more detailed subset of the larger elevation range discussed by Cohen and Small (1998). To some extent, the population distributions are dictated by the available land area at each elevation and distance from coastline. Figure 5 shows that land area also diminishes with elevation and distance from coastline. There is more land available at the periphery of a continent than in the interior as a simple result of geometry. There is also more land area near sea level than at higher elevations because erosional and depositional processes constantly transport tectonically uplifted material to lower elevations near sea level. This is less apparent over the 100-m range of elevations shown in Figure 5 than over the 4000-m range of elevations discussed by Cohen and Small (1998).

Because the distribution of population is constrained by the distribution of land area (assuming that the number of people living on boats is negligible), it is informative to normalize distributions of population with distributions of available land area to produce estimates of Integrated Population Density (IPD) (Figure 5). Even when available land area is taken into account, the low coastal elevations are still more heavily populated than are the higher continental interiors. The total number of people per square kilometer of avail-

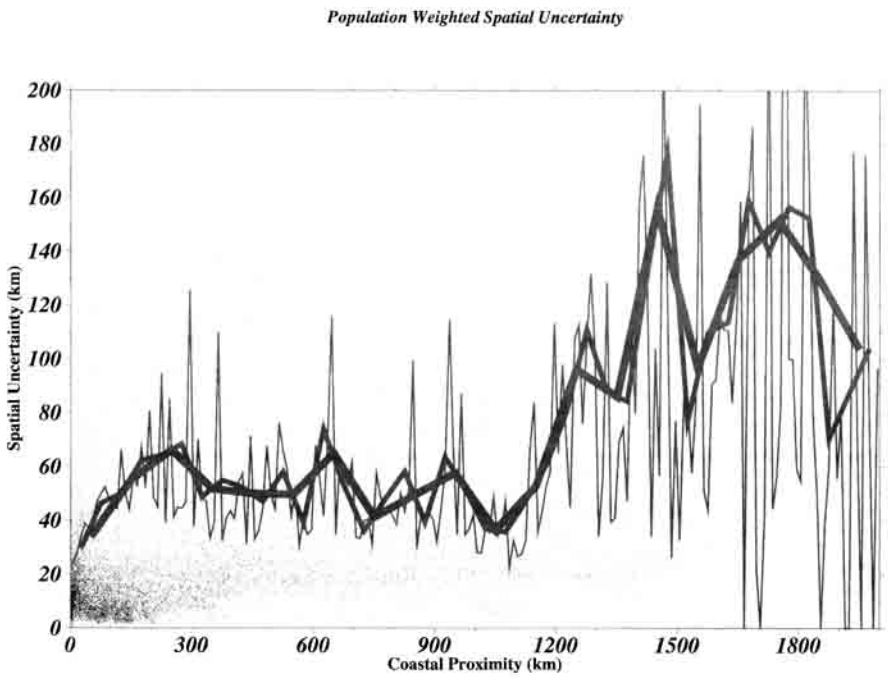

Figure 4: Distribution of spatial uncertainty of the population data as function of coastal proximity. Points show individual spatial uncertainty ([square root(area)]/2) of 19,032 census data compiled by Tobler et al. (1997) and shaded curves show population-weighted mean uncertainty in 10- (thin curve), 50-, and 100-km-wide distance bins. Mean spatial uncertainty is generally less for coastal census tracts but is still on the order of 30 km.

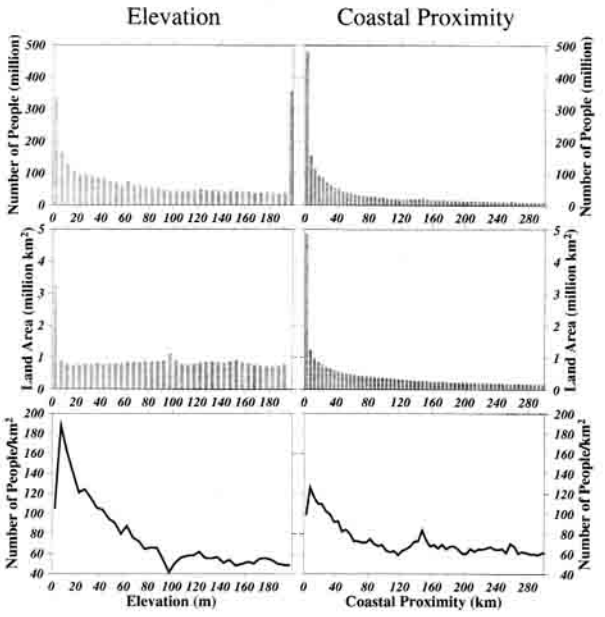

Figure 5: Estimates of the distribution of population and populated land area as a function of elevation and coastal proximity. Population diminishes rapidly with increasing elevation and increasing distance from coastline but is constrained by the land area available for habitation. Dividing the total population occupying a particular elevation (or distance) by the total land area available at that elevation (or distance) gives estimates of integrated population density (IPD) as a function of elevation or coastal proximity. Both IPD estimates verify that coastal areas and low elevations are more heavily populated than are higher inland areas. Integrated densities diminish most rapidly within 100 m of sea level and 100 km of coasts.

able land diminishes rapidly within 100 m of sea level and 100 km of the coast (Figure 5). The relatively large values for land area and population in the lowest and most coastal bins in these histograms partly reflect the fractal dimension of the coastline at the 5′ grid resolution. Consequently, the drops in IPD in these bins may result from the relatively large number of sparsely populated coastal pixels in areas with convoluted coastlines and numerous small islands like Patagonia and the Canadian Arctic. This reflects an inherent shortcoming of studies that combine densely and sparsely populated areas in a single analysis.

Many coastal areas contain mountainous topography (e.g., California) and many low lying basins do not occur near coastlines (e.g., Death Valley); thus, it is necessary to consider elevation and coastal proximity together when discussing populations at risk of coastal hazards. This is possible because each population estimate is associated with a specific elevation and distance from coastline. Figure 6 provides estimates of the cumulative number of people within a given distance of a coastline and below a given elevation. Approximately 400 million people live within 20 m of sea level and within 20 km of a coast worldwide. In light of the uncertainties discussed above, the accuracy of this number is obviously questionable. With more accurate population and elevation data at higher spatial resolution, this type of plot could provide estimates of the number of people at risk for different coastal hazard or SLR scenarios. It is not possible to make meaningful estimates of population or land area at risk from coastal hazard using the plot shown in Figure 6 because of the magnitude of the uncertainties discussed above. However, the plot does quantify the extent to which human populations tend to occupy coastal regions relative to continental interiors.

DISCUSSION

Certain caveats must be kept in mind when interpreting these results. The most obvious caveat is the uncertainty

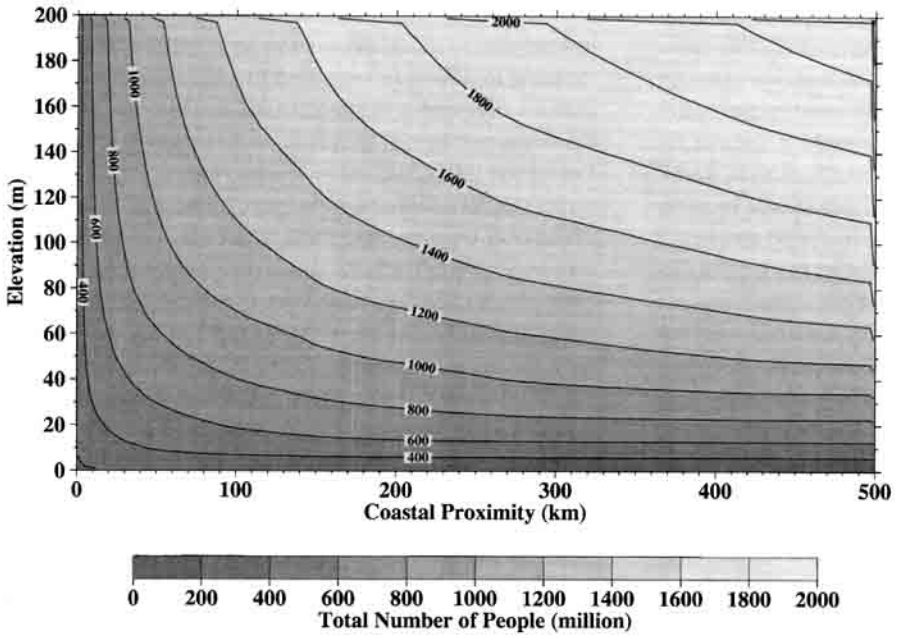

Figure 6. Estimate of the cumulative global population within a range of elevations and coastal proximities. Contours indicate total number of people both within a given distance from the nearest coast and also within a given elevation above mean sea level.

discussed in the previous section. The data in the histograms are shown in increments of 5 m of elevation and 5 km of distance but Figure 4 indicates spatial uncertainties of >20 km for population in districts nearest coastlines. This does not account for uncertainties in the elevation model or in the population counts.

The histograms shown here represent a possible but not necessarily probable distribution of people and land area within the limits of the uncertainties of the data sets. The gridded population estimates were used to construct these histograms so the assumption of uniform spatial distribution within census districts is implicit in these histograms. Uniform population distribution seems unlikely at the scale of this analysis so the distributions shown here represent the limiting case of the range of possible distributions allowed by the district-level data. Taken together, the spatial uncertainty in population distribution combined with the spatial localization implied by the proximity distribution compounds the difficulty of making meaningful estimates. If the population distribution implied by the data were more uniformly distributed with respect to coastal proximity, the implications of the uncertainty would be less significant. As it stands, the uncertainty associated with the lower resolution census data combined with the localization implied by the higher resolution census data suggest a wider range of possible distributions than would be expected if the higher resolution data were more uniform.

In spite of the uncertainties, this study gives some indication of the populations at low elevations near coasts relative to the populations in the interiors of continents. Even if these data do not provide precise estimates of numbers of people at risk of coastal hazards, they do indicate which locations require more detailed data. Integrated population density apparently diminishes most rapidly within 100 km from a coast and 100 m above sea level; within this zone, the populations may be more localized than indicated by these results. Further investigation at different spatial scales may be warranted. It would be interesting, for instance, to know whether regional population distributions show a similar pattern and if the spatial scaling is modulated by other climatic variables (see Small and Cohen, 1999, and http://www.ldeo.columbia.edu/~small/population.html, for a discussion of climatic variables). Some of these questions can be investigated using subsets of the data presented here, but in many areas data of higher resolution and greater accuracy are required. Cross-cultural similarities in spatial population distribution, related to fundamental environmental factors, are conceivable and potentially important.

Qualitatively, this study confirms that large numbers of people live at low elevations near coasts. However, the principal contribution of the study is to show that the available data are inadequate to permit quantitatively precise estimates of the number of people likely to be affected by possible levels of SLR or storm surges in coastal areas on a global basis. The lack of adequate data means that it is impossible to anticipate with useful precision the number of people who could be affected by alternative scenarios of climatic change. Without such numbers, it is difficult to plan for adaptive responses or to evaluate how much it would be worth to invest in preventive measures. If SLR has the potential to cause substantial global effects, it would be sensible to invest more resources in more accurate, higher resolution data on the spatial distribution of the human population and elevation in coastal areas. Of the two, elevation is, by far, the simpler to measure. Airborne and satellite-based radar and laser altimeters are now capable of mapping coastal topography and its changes at resolutions far greater than the data used in this study. Satellite observations of land cover changes in coastal zones also provide a means to quantify changes in coastal habitation (although not population) at resolutions high enough to serve a number of purposes (Leatherman, 1993).

Uncertainties in climate change scenarios are compounded by the limited distribution of coastal sea level observations. Figure 2 shows that in areas where detailed, long-term observations have been made (Figure 1), the magnitude of the local effects (subsidence, tidal amplitude, etc.) are larger than is the absolute magnitude of global mean SLR resulting from existing climate change scenarios. The majority of long-term (>30 years) monitoring stations are located in Europe and North America but the largest and most rapidly growing populations potentially affected by coastal hazards are located in southern and eastern Asia. Efforts to understand global scale climate change need to be accompanied by studies of the local and regional factors that magnify, or moderate, their impact on coastal populations.

This analysis shows that estimates of the 1994 global low-elevation coastal population are highly uncertain. Attempting to project future global low-elevation coastal populations compounds the uncertainty for three reasons. First, the future numbers of people in each country are uncertain. During the 1990s, successive United Nations Population Division middle estimates of the population in 2050 have declined over time, because fertility rates in some developing countries have fallen faster than anticipated, and in some regions, death rates have risen unexpectedly. For example, between the 1996 and the 1998 United Nations projections, the estimated population in 2050 fell by ~0.5 billion people (United Nations, 1998a, 1998b). Second, the middle estimates, typically used in projections of climatic effects of anthropogenic atmospheric emissions, are flanked above and below by widening bands of uncertainty ("high" and "low" projections, which are themselves uncertain). The uncertainty in the number of people who will be contributing greenhouse gases and sulfate emissions is usually neglected in the scenarios used as inputs to GCM models. Third, the

future spatial distribution of the population within each country is at least as uncertain as, and probably more uncertain than, the future total population of that country. The rate of urbanization will strongly affect the size of the low coastal population in many countries where major cities are near sea coasts. For these three reasons, precise quantitative forecasts of how many people will be exposed to coastal hazards half a century hence may be hazardous themselves, although it is clear that the numbers of people at risk could be large.

ACKNOWLEDGMENTS ●

This work was funded, in part, by the Columbia Earth Institute of Columbia University. C. S. gratefully acknowledges the support of the University Consortium for Atmospheric Research (UCAR) Visiting Scientists Program and the Columbia Earth Institute. V. G. acknowledges the generous support of the National Aeronautics and Space Administration Cooperative Agreement with Columbia University on Interdisciplinary Research on Climate Variability and the Impacts Associated with Regional Climate Change. J. E. C. acknowledges the support of U. S. National Science Foundation grant BSR92-07293 and the hospitality of Mr. and Mrs. William T. Golden.

REFERENCES ●

Cohen, J. E., and Small, C. (1998). Hypsographic demography: The distribution of the human population by altitude. *Proc Nat Acad Sci USA, 95*, 14009–14014.

Cohen, J. E., Small, C., Mellinger, A., Gallup, J., and Sachs, J. D. (1997). Estimates of coastal populations. *Science, 278*, 1211–1212, 1214.

Douglas, B. (1991). Global sea level rise. *J Geophys Res, 96*, 6981–6992.

Gornitz, V. (1995a). A comparison of differences between recent and late Holocene sea level trends from eastern North America and other selected regions. *J Coast Res, 17*, 237–297.

Gornitz, V. (1995b). Monitoring sea level changes. *Climate Change, 31*, 515–544.

Gornitz, V., and Seeber, L. (1990). Vertical crustal movements along the East Coast, North America, from historic and Holocene sea level data. *Tectonophysics, 178*, 127–150.

Hansen, J., Russell, G., Rind, D., Stone, P., Lacis, A., Lebedeff, S., Ruedy, R., and Travis, L. (1983). Efficient three-dimensional global models for climate studies: Models I and II. *Monthly Weather Revs, 111*, 609–662.

Hansen, J., Fung, I., Lacis, A., Rind, D., Lebedeff, S., Ruedy, R., and Russell, G. (1988). Global climate changes as forecast by Goddard Institute for Space Studies three dimensional model. *J Geophys Res, 93*, 9341–9364.

Hoozemans, F. M. J., Marchand, M., and Pennekamp, H. A. (1993). Sea level rise: A global vulnerability assessment. The Hague, The Netherlands; Delft Hydraulics.

Houghton, J. T., Callander, B. A., and Varney, S. K. (Eds.) (1992). *Climate change 1992: The supplementary report to the IPCC scientific assessment*. Cambridge: Cambridge University Press.

IPCC 1995. (1996a). Changes in sea level. In J. T. Houghton, L. G. Meira Hilho, B. A. Callander, et al. (Eds.), *Climate change 1995: The science of climate change* (pp. 359–405). Cambridge: Cambridge University Press.

IPCC 1995. (1996b). Coastal zones and small islands. In R. T. Watson, M. C. Zinyowera, and R. H. Moss (Eds.), *Climate change 1995: Impacts, adaptations and mitigation of climate change: Scientific-technical analyses* (pp. 289–324). Cambridge: Cambridge University Press.

Leatherman S. P. (1993). Coastal change. In R. J. Gurney, J. L. Foster, C. L. Parkinson (Eds.), *Atlas of satellite observations related to global change* (pp. 327–340). Cambridge: Cambridge University Press.

National Oceanographic and Atmospheric Administration (NOAA). (1995). Tide tables for east coast of North and South America including Greenland. Washington DC: National Ocean Service.

Nicholls R. J., and Leatherman S. P. (Eds.) (1995). Potential impacts of accelerated sea-level rise on developing countries. *J Coastal Res.* 14:1–14.

Oppenheimer, M. (1998). Global warming and the stability of the West Antarctic Ice Sheet. *Nature, 393*, 325–332.

Russell, G. L., Miller, J. R., and Rind, D. (1995). A coupled atmosphere-ocean model for transient climate change studies. *Atmosphere-Ocean, 33*, 683–730.

Small, C., and Cohen, J. E. (1999). Continental physiography, climate and the global distribution of human population. In *Proceedings of the International Symposium on Digital Earth* (pp. 965–971). Beijing: Science Press.

Spencer, N. E., and Woodworth, P. L. (1993). *Data holdings of the Permanent Service for Mean Sea Level, PSMSL*. Birkenhead, UK: Bidston Observatory.

Tobler, W., Deichmann, U., Gottsegen, J., and Malloy, K. (1997). World population in a grid of spherical quadrilaterals. *Intl J Population Geogra, 3*, 203–225.

United Nations. (1998a). *World population prospects: The 1996 revision*. United Nations Publication New York: ESA/P/WP.138.

United Nations. (1998b). *World population prospects: The 1998 revision*. United Nations Publication New York: ESA/P/WP.150.

Wessel, P., and Smith, W. H. F. (1996). A global self-consistent, hierarchical, high-resolution shoreline database. *J Geophys Res, 101*, 8741–8743.

ABOUT THE AUTHORS ●

Christopher Small

Dr. Small is an associate research scientist and lecturer at the Lamont Doherty Earth Observatory of Columbia University. He holds a Ph.D. in Earth Sciences (geophysics) from the Scripps Institution of Oceanography, University of California–San Diego as well as degrees from the University of Texas at Austin and the University of Wisconsin–Madison. His research interests focus on the evolution and structure of ocean basins and on applications of remote sensing to studies of continental physiography and population distribution.

Joel E. Cohen

Joel E. Cohen is Abby Rockefeller Mauzé Professor of Populations at Rockefeller University and Professor of Populations at Columbia University in New York City. In 1999, Cohen was co-winner of the Tyler World Prize for Environmental Achievement. In 1997, he won the first Olivia Schieffelin Nordberg Prize given by the Population Council "for excellence in writing in the population sciences." The prize was given for his book, How Many People Can the Earth Support? (W. W. Norton, 1995). Cohen is an elected member of the American Academy of Arts and Sciences, the American Philosophical Society, and the U.S. National Academy of Sciences.

Vivien Gornitz

Vivien Gornitz received her Ph.D. in Geology from Columbia University in 1969. As a Research Scientist at Goddard Institute for Space Studies and Columbia, she investigates historic sea level trends and impacts of future sea level rise on the coastal zone.